J Neurophysiol 94: 1212–1224, 2005.
First published April 27, 2005; doi:10.1152/jn.01295.2004.

Error Parsing in Visuomotor Pointing Reveals Independent Processing of Amplitude and Direction

Philippe Vindras,[1,2] Michel Desmurget,[3] and Paolo Viviani[1,4]

[1]*Faculty of Psychology and Educational Sciences, University of Geneva, Geneva, Switzerland;* [2]*Department of Neurology, Neurological Hospital Pierre Wertheimer, Bron, France;* [3]*Space and Action, Institut National de la Santé et de la Recherche Médicale, Bron, France; and* [4]*Faculty of Psychology, Vita-Salute San Raffaele University, Milan, Italy*

Submitted 17 December 2004; accepted in final form 14 April 2005

Vindras, Philippe, Michel Desmurget, and Paolo Viviani. Error parsing in visuomotor pointing reveals independent processing of amplitude and direction. *J Neurophysiol* 94: 1212–1224, 2005. First published April 27, 2005; doi:10.1152/jn.01295.2004. An experiment investigated systematic pointing errors in horizontal movements performed without visual feedback toward 48 targets placed symmetrically around two initial hand positions. Our main goal was to provide evidence in favor of the hypothesis that amplitude and direction of the movements are planned independently on the basis of the hand-target vector (vectorial parametric hypothesis, VP). The analysis was carried out mainly at the individual level. By screening a number of formal models of the potential error components, we found that only models compatible with the VP hypothesis provide an accurate description of the error pattern. A quantitative analysis showed that errors are explained mostly by a bias in the represented initial hand position (46% of the sum of squared errors) and a visuomotor gain bias (26%). Range effect (3%), directional biases (3%), and inertia-dependent amplitude modulations (1%) also provided significant contributions. The error pattern was incompatible with the view that movements are planned by specifying either a final posture or a final position. Instead, the results fully supported the view that, at least in the horizontal plane, amplitude, and direction of pointing movements are planned independently in a hand- or target-centered frame of reference.

INTRODUCTION

To plan reaching hand movements, the CNS must map information about the initial arm posture and the target position into an appropriate pattern of muscular activity. There are two main views on the nature of this complex transformation. According to the *postural control* view (Bizzi et al. 1984; Desmurget and Prablanc 1997; Feldman 1966; Flanders et al. 1992; Rosenbaum et al. 1995), the target position is first transformed into a desired arm posture, which is then used to compute the motor commands. By definition, all the models that adopt this view postulate that the distribution of end points for a given target is *independent* of the initial position. According to the *vectorial parametric* (VP) view (Atkeson and Hollerbach 1985; Bock and Eckmiller 1986; Ghez et al. 1997; Rossetti et al. 1995; Vindras and Viviani 1998), the CNS computes the hand-target vector and then plans the motor commands by processing independently amplitude and direction of this vector. The VP hypothesis predicts that the distribution of the end points is *dependent* on the initial position. However, it places strong constraints on the nature of this dependence inasmuch as it postulates that the initial position affects *only* the computation of the hand-target vector, whereas the transformations of this vector into motor commands are *independent* from the initial position. Converging evidence supports the VP hypothesis: changes in visuomotor gain are compensated more easily than changes in direction and generalize to all directions (Bock 1992; Krakauer et al. 2000; Vindras and Viviani 2002); imposed biases in the transformation between target and movements directions remain invariant in extrinsic space independently of the initial hand position (Krakauer et al. 2000); and RT studies suggest that movement extent and direction are specified independently (Bock and Arnold 1992; Desmurget et al. 2004; Ghez et al. 1997; Rosenbaum 1980). However, there is still no direct demonstration that the transformation of the hand-target vector is independent of the initial position.

The debate between these contrasting views revolves mainly around the origin of pointing errors. In the case of planar horizontal movements, the distribution of the variable errors is elongated in the direction of the hand-target vector (Desmurget et al. 1997; Gordon et al. 1994b; Messier and Kalaska 1999; Vindras and Viviani 1998). Alternatively, in the case of three-dimensional movements, some authors (e.g., Flanders et al. 1992) reported a pattern of errors consistent with a shoulder-centered frame of reference and argued that errors are due to approximations in the sensorimotor transformation from target position to desired arm posture. It has also been claimed that—at least in the case of memorized targets—the distribution of errors originates from the representation of the target within a frame of reference centered on the eye (McIntyre et al. 1997, 1998).

The primary goal of this study is to demonstrate that an in-depth analysis of individual pointing errors provides strong evidence in favor the VP hypothesis. The demonstration hinges around the notion that the transformation of the perceived hand-target vector in motor commands ought to be independent of the initial position (see preceding text). Specifically, we tested whether constant errors can be factored out into four components predicted by the VP hypothesis: *initial-position bias* due to an inaccurate representation of the hand position (Vindras et al. 1998); *scaling biases* and *directional biases,* both arising independently at the level of the sensorimotor transformation; and *inertia-dependent amplitude biases* caused by the directional anisotropy of arm inertia (Gordon et al. 1994a). According to the VP hypothesis, these components should follow a specific pattern. Initial-position biases may de-

Address for reprint requests and other correspondence: P. Viviani, University of Geneva, Faculty of Psychology and Educational Sciences, 40, Bd Pont d'Arve, Geneva, CH-1205, Switzerland (E-mail: Paolo.Viviani@pse.unige.ch).

The costs of publication of this article were defrayed in part by the payment of page charges. The article must therefore be hereby marked "*advertisement*" in accordance with 18 U.S.C. Section 1734 solely to indicate this fact.

pend on the hand location within the workspace (Vindras et al. 1998) but should be independent of the amplitude and direction of the movement. Scaling biases should be independent of the initial position and of the movement direction except as a result of the directional anisotropy of arm inertia. Finally, directional biases should be independent of movement amplitude. We tested whether these constraints are satisfied. We also tested for the presence of other sources of errors that are either inconsistent with or not predicted by the VP hypothesis.

Finally, to strengthen the case for the VP hypothesis, we also tested on a limited set of results the key prediction, common to all postural models, that final position is independent of the initial position.

METHODS

Subjects

Ten right-handed adults, eight women and two men, with ages ranging from 21 to 43 yr, participated to the experiment for payment. Subjects were naive with respect to the purpose of the experiment. They had normal or corrected-to-normal vision and presented no evidence of neurological disorders. The experimental protocol was approved by the Ethical Committee of the University of Geneva. Informed consent was obtained from the subjects.

Apparatus and task

Subjects sat in front of a horizontal digitizing tablet (model No. 2200–2436, Numonics, Montgomeryville, PA; size: 110 × 80 cm, resolution: 0.0025 cm, sampling rate: 200 Hz), which defined the work-plane (Fig. 1). We adjusted individually the height of the chair, and asked the subjects to bring the chest in contact with the tablet edge. The shoulder was ~20 cm above the tablet, and the forearm was approximately horizontal. Subjects held the recording stylus (length: 20 cm, diameter: 1 cm, weight: 20 g) with the right hand. A pair of galvanometric mirrors controlled the position of a laser spot (diameter: 0.4 cm) projected on a dimly illuminated translucent board located 60 cm above the tablet. The spot identified the required initial position of the hand and the target. A half-reflecting mirror was positioned horizontally between the pointing surface and the translucent board. Looking from above the mirror, subjects perceived the virtual image of the spot on the work-plane. A light source was placed between the work plane and the mirror. When the light was on, subjects could see both the spot and their hand. When the light was off, only the laser spot remained visible. The room where the experiment took place was kept in total darkness. The controlling computer switched on and off the light source according to the stylus position (see following text). The experimenter monitored the instantaneous position of both the stylus and the laser spot. At the beginning of each trial, he helped the subject to place the tip of the stylus on the initial position with a 1-mm precision.

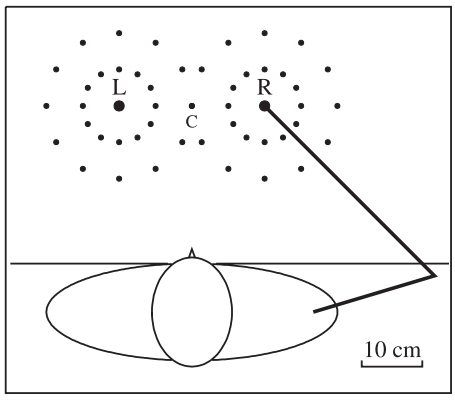

FIG. 1. Experimental set-up. Twenty-four targets were positioned around a left (L) and right (R) initial position, respectively. Inner targets were at 6 cm form the center, outer targets at 12 cm. Targets to the left (right) of the midline were reached from initial position L (R). The only common target C was reached from both initial positions. The work plane was at the height of the sternum.

There were two initial positions (L and R) located symmetrically 12 cm to the left and to the right of the subjects' sagittal plane at 26 cm from the edge of the tablet. There were four sets of targets, each including 12 locations equally spaced along the circumference of a circle. Two sets were centered on position L, at a distance of 6 and 12 cm. The other two sets were centered on position R at the same distances (Fig. 1). The experiment included a pointing task and a localization task. Results from the localization task, which did not involve hand displacements, have been published (Vindras et al. 1998). This article deals only with the pointing task, which consisted of reaching the target position selected by the laser spot from one of the two starting positions. Subjects were instructed to point "as accurately as possible, with a single, uncorrected movement." Movements were to start as soon as the target appeared, but we did not insist on minimizing the reaction time.

Pointing trials included three steps. *1*) The experimenter guided the subject's hand to one of the two initial positions (L or R). The hand remained visible during the first part of this placing operation to compensate for possible proprioceptive drifts (Wann and Ibrahim 1992). The light was switched off when the tip of the stylus was within 4 cm from the required position, preventing the subject from estimating visually the initial position of their hand. *2*) The target spot was turned on, and the subject moved the stylus toward the target. To minimize corrective feedback, the target was turned off 200 ms after hand movement onset, roughly at the time of peak acceleration (Prablanc et al. 1986). *3*) The experimenter moved the hand away from its current location (≈30 cm), and the light was turned on. Thus subjects were never allowed to compare the estimated and actual hand positions at the end of the movement.

The experiment involved a total of 144 trials: 96 pointing trials [2 (starting position) × 12 (direction) × 2 (distance) × 2 (repetition)] and 48 localization trials. The first 72 trials consisted of one pointing toward each of the 48 targets and 24 localizations. Pointing and localization trials were intermixed in a pseudorandom order. The order of target presentation was also randomized. The same sequence was replicated for the remaining 72 trials. Before the experiment, subjects were trained until they felt comfortable with both the task and the apparatus. On average, the familiarization phase involved 10 trials. A complete session lasted ~1 h.

Data analysis

We recorded the x and y coordinates of the position of the stylus for 1.5 s starting at the time of target presentation. Before computing velocity and acceleration, the data were filtered and differentiated twice using an optimal FIR algorithm (Rabiner and Gold 1975) (cutoff frequency: 8 Hz). Movement onset was identified automatically as the first time velocity exceeded 1 cm/s and remained above this threshold for ≥50 ms (across subjects, peak velocity ranged between 35 and 72 cm/s). Likewise, the end of the movement was defined as the first time velocity remained for 100 ms below 1 cm/s. The pointing error was defined as the vector from the target to the final position of the stylus. We also computed the duration of the movement as well as the value and timing of peak velocity and peak acceleration. All subsequent analyses were performed on the average of these measures for the two repetitions of each trial (analyzing single trials would have prevented us from assuming the independence of unaccounted residuals; see RESULTS). Movement amplitude and direction were defined by the vector between initial and final positions.

RESULTS

Different sources of inaccuracy

To test whether pointing errors can be factored out as predicted by the VP hypothesis, we considered a class of models all of which assume that pointing movements are affected by an idiosyncratic combination of four sources of inaccuracy. Figure 2 illustrates schematically the effect of each type of inaccuracy on the pattern of pointing errors. The figure also indicates the order with which the biases are assumed to come into play (directional and scaling biases commute). Note that the order influences the final result. However, we checked that as long as the first source of error was not large, the effect was small because the targets were placed symmetrically.

First Fig. 2, *1*, the hand-target vector may be biased by an erroneous representation of the initial hand position with respect to the targets. If this was the only source of error, the pattern of final positions (arrowhead) would be simply a copy of the target layout shifted by the same amount (and in the opposite direction) as the vector from the actual (□) to the represented initial position (○). The initial-position bias may vary as a function of the hand starting point because the ability to locate the hand at rest varies with the posture of the arm (Cruse 1986; Vindras et al. 1998).

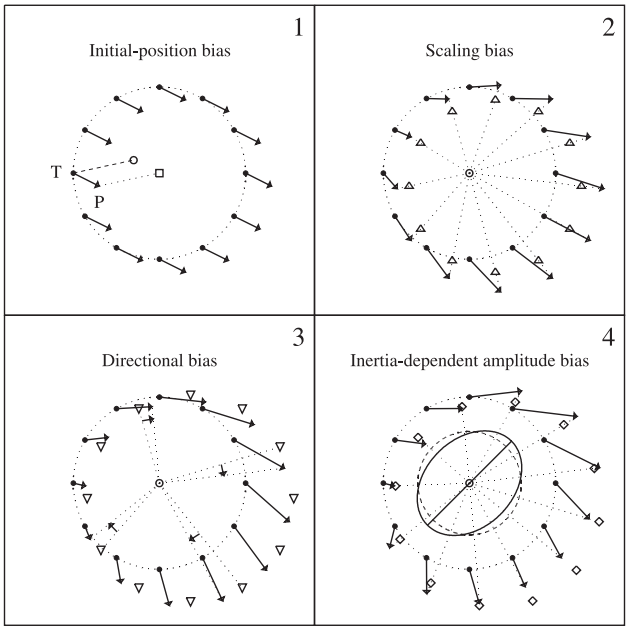

FIG. 2. Modeling the biases. The mapping of the targets into the actual final positions is decomposed into 4 steps, each 1 of which adds a different error component. *1*: initial-position errors are represented by a parallel displacement of all targets. The displacement vector is supposed to correspond to an opposite bias in the represented hand position (○). For example, the final position in pointing to target T is in P because the subject executes a movement equal to the represented hand-target vector (- - -) from the actual (□), not the represented (○) hand position. *2*: direction-independent amplitude errors originate from an inaccurate transformation of the hand-target distance into movement extent. The function that maps target distance into movement extent may be a constant visuomotor gain (as in the example illustrated; gain: 1.20), or a more complex, distance-dependent transformation (see Table 1). As shown in the panel, this transformation acts on the final positions predicted after step 1 (△). *3*: direction errors result from a uniform rotation of the final positions predicted after step 2 (▽) around the biased initial position (in the example, 10°). *4*: direction-dependent amplitude errors are modeled by an elliptic modulation of the distance of the position after step 3 (◇) from the biased initial position. The axes of the ellipse are aligned with the axes of the inertial tensor of the arm. →, the predicted pattern of pointing errors. The errors injected in steps 3 and 4 have been emphasized for the sake of clarity with respect to their actual importance. Note that the 4 steps of the modeling procedure do not commute except for steps 2 and 3.

The second source of inaccuracy (scaling bias; Fig. 2, *2*) affects the transformation from hand-target distance to movement amplitude. The new final positions result from transforming in a systematic manner the distance from the biased hand position (○) to the target (△). In the example of Fig. 2, distances are transformed by a single multiplicative factor (visuomotor gain). In a more elaborate model, the transformation is an affine function, which implies that the gain depends on the distance (range effect) (Slack 1953). We also consider other (nonlinear) transformations as well as the case in which the gain depends on the initial position. Note that this latter possibility is at variance with the VP hypothesis.

The third source of inaccuracy (directional bias; Fig. 2, *3*) affects the transformation from the target direction to the direction of the movement. The new final positions result from rotating the previous ones (▽) around the biased hand position. In the example of Fig. 2, the rotation is rigid (10° clockwise). We explored also the case (again at variance with the VP assumption that movement amplitude and direction are planned independently) in which the extent of the rotation depends on target distance.

The fourth source of inaccuracy (inertia-dependent amplitude bias; Fig. 2, *4*) originates from the execution phase. As reported in earlier studies (Gordon et al. 1994a), the directional anisotropy of the arm inertia may result in direction-dependent modulations of movement amplitude. This possibility is exemplified in the figure where distances are increased or decreased according to an elliptic profile centered on the biased hand position. The long axis of the ellipse is supposed to be aligned with the axis of least inertia of the arm.

Figure 3 shows the complete results from two subjects to illustrate the great variety of behaviors that the VP hypothesis is expected to encompass. In one subject (*MO*), the distribution of the pointing errors (*bottom*) followed almost exactly a centripetal pattern, the average errors (central arrows) being almost zero. Such a distribution shows that scaling biases were predominant in this subject. By contrast, in another subject (*KA*), pointing errors were fairly parallel for both initial positions. The main source of inaccuracy in this individual appears to be a biased representation of the initial hand position.

In other subjects, the pattern of pointing errors was more complex than the examples in Fig. 3. Figure 4 outlines, for one representative case (*KO*), the procedure followed to factor out the sources of inaccuracy according to the general model described above. Additional details will be provided when the contribution of each source is analyzed quantitatively. Starting from the vectors from the initial position to the targets, we computed an increasingly accurate description of the actual movements by adding the error components corresponding to each source of bias, in the sequence indicated in Fig. 2. *C* shows the actual errors (vector from the target to the actual end point). At each step (*D–F*), the squared residuals (vectors from the predicted to the actual end points) were summed over all targets (SSE). Then, the parameters of all the components included in the model were estimated anew by minimizing the SSE at that step.

First, we added to each hand-target vector a best-fitting constant vector (i.e., the average of all pointing errors). In this example (Fig. 4), the first step transforms the actual errors (*C*) into a centripetal pattern (*D*) similar to the one for s*ubject MO* (Fig. 3). Note that the extreme skew of the trajectories for the

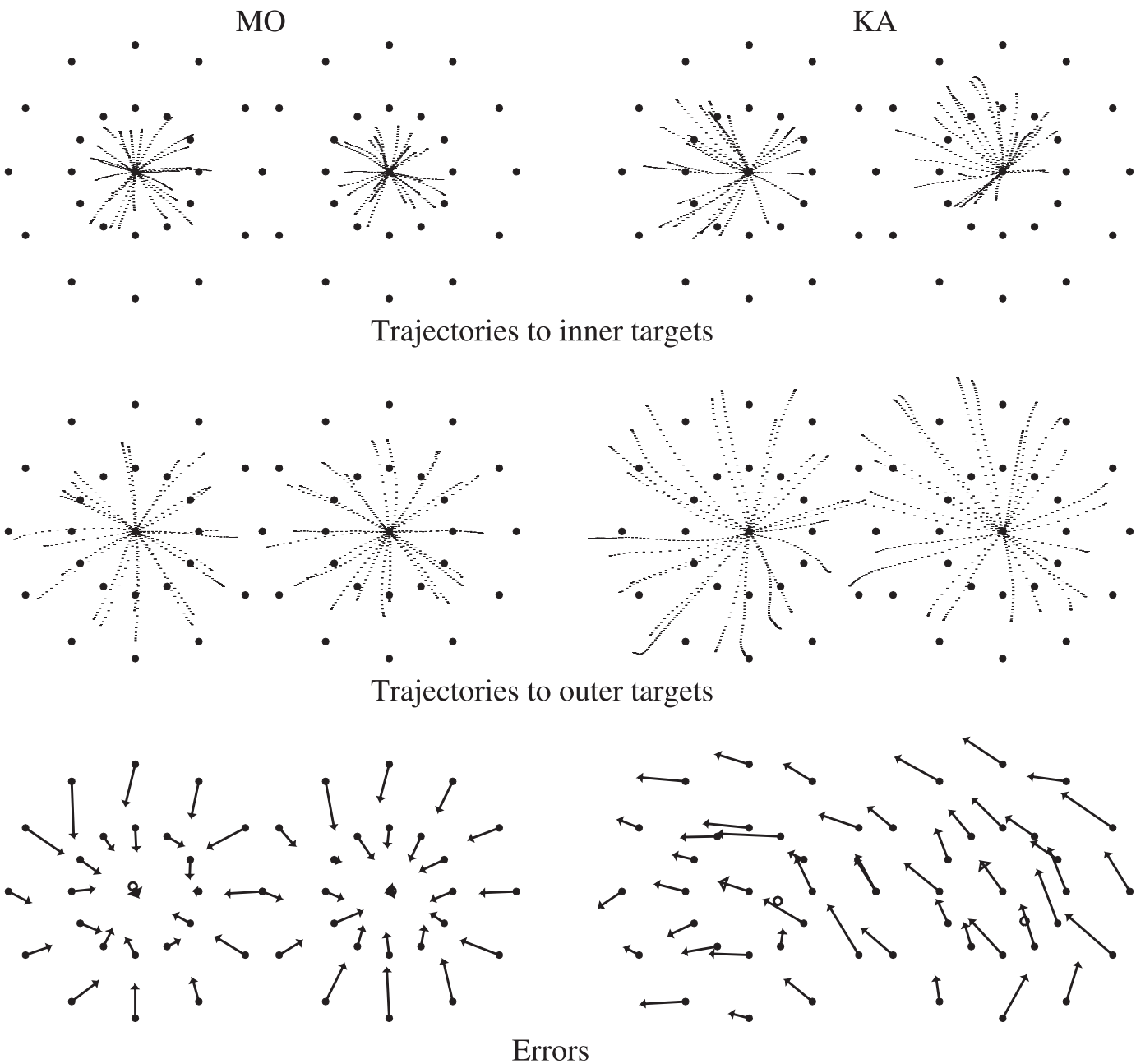

FIG. 3. Movement trajectories and errors. Results from the 2 subjects (*MO* and *KA*) whose behavior reflected mostly 2 different sources of inaccuracy. *Top* and *middle*: sampled trajectories to inner and outer targets, respectively (2 trials for each target). *Bottom*: error vectors from targets to movement end points (average of 2 trials). The radial pattern of errors of *MO* indicates a large, systematic undershooting of the targets. The pattern of errors of *KA* is dominated by a large bias in the represented initial position of the hand (empty circle). *Bottom, right*: reported in a different format data from Vindras et al. (1998).

left initial position (*A*) is accounted for almost entirely by the hypothesis of a biased representation of the initial position. In the following step, we introduced the scaling bias by altering in a principled way the amplitude of the movement predicted at the end of the first step. Typically, the resulting pattern of residuals still contained small but identifiable counterclockwise directional components (*E*). In the third step, we introduced the directional bias by rotating the movement vectors predicted in the second step. Finally, we introduced the fourth error component, which describes the effects of the directional anisotropy of the arm inertia. The unaccounted residuals after this procedure (*F*) were fairly unsystematic. For the subject whose results are shown in Fig. 4, unaccounted residuals totaled 11.2% of the initial SSE. By comparison, initial-position, scaling, directional and inertia-dependent biases, accounted for 65.5, 20.6, 2.6, and 0.1% of the initial SSE, respectively.

Testing the adequacy of different four-component models

We derived specific models from the four-component general scheme outlined above by stipulating the relationship between the error components and the relevant experimental variables. Table 1 lists the candidate models that were tested along with the conventional names with which they are referred to. The parameters in the equations describing the models are allowed to depend on the initial position. All

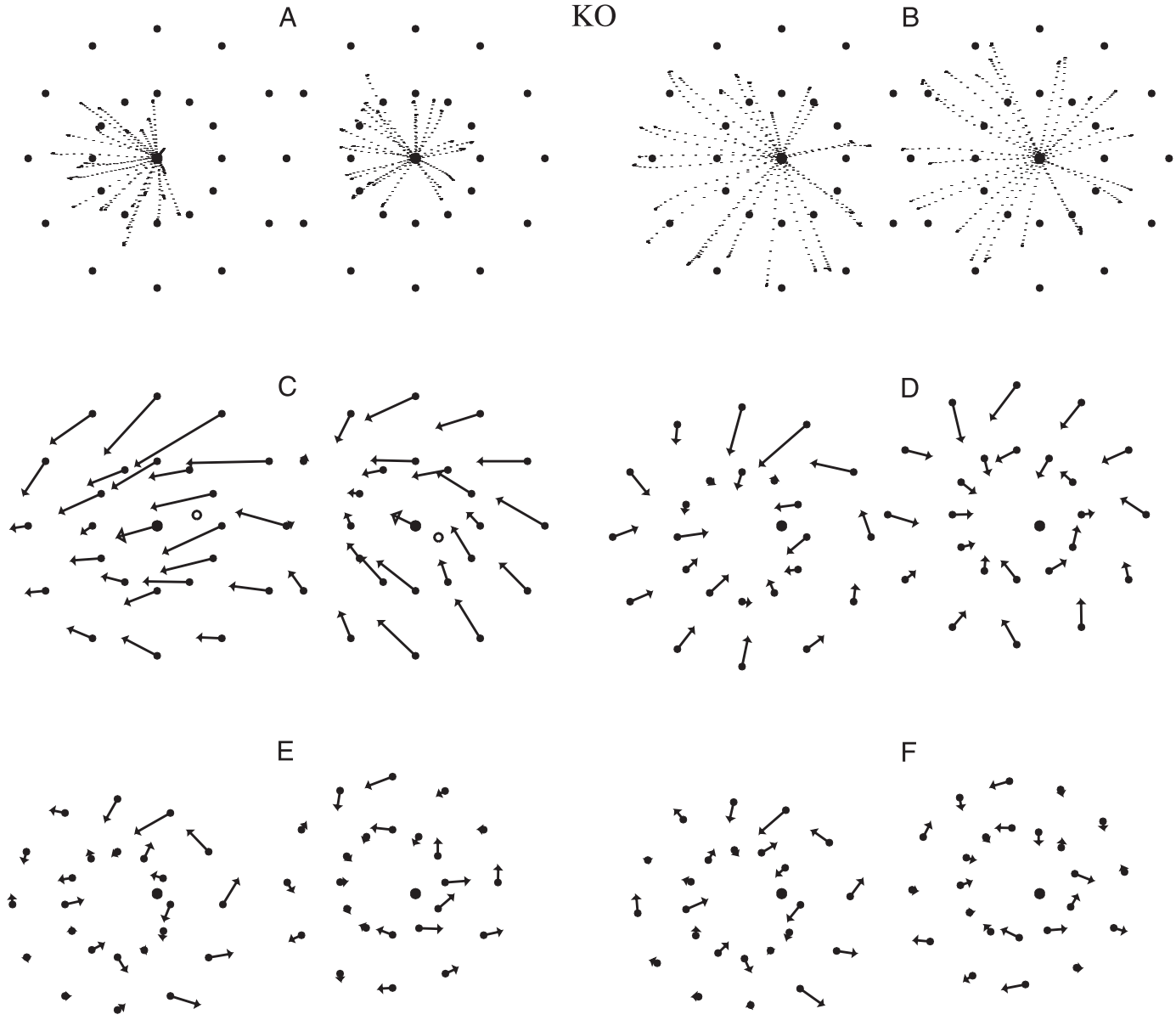

FIG. 4. Modeling the errors. Results from 1 representative subject (*KO*). *A* and *B*: sampled trajectories to inner and outer targets, respectively (2 trials). The large filled circle in *C–F* indicates the actual initial hand position. The empty circle in *C* indicate the represented initial position of the hand. *C*: error vectors from *targets* (small dots) to movement end points (average of 2 trials). *D–F*: vectors from the *predicted* (small dots) to the actual end points at successive steps of the modeling procedure. *D*: residuals after taking into account the bias in the represented initial position of the hand. *E*: residuals after accounting for scaling biases. *F*: unaccounted residuals. For simplicity, the 2 steps of the procedure by which the small directional and inertia-dependent biases are added are not detailed.

models were tested twice, once by fitting a single set of parameters to the data for both initial positions (1 fit) and once by allowing the parameters to depend on the initial position (2 fit). The reason for this procedure is that obtaining a significantly better approximation to the data with two fits (i.e., twice as many parameters) than with one fit may signal a violation of the VP hypothesis. The logic of the test consisted of demonstrating that models that include degrees of freedom not predicted by the VP hypothesis fare no better than those consistent with the hypothesis. Thus for instance, a model allowing scaling biases to depend on the hand initial position is discarded unless it accounts for a significantly larger amount of SSE than a model in which errors are independent of the hand initial position.

Comparison between models was carried out both at the individual and at the sample level. For individual data, the comparison involved F tests. Assuming that the x and y components of the residuals at the 48 targets are 96 independent Gaussian variates with null mean and common variance, the SSE for a model with n parameters has a χ^2 distribution with $96 - n$ df. Given two models M_i and M_j with n_i and n_j parameters ($n_i < n_j$) and with SSE S_i and S_j ($S_i > S_j$), the random variable $F = [(S_i - S_j)/(n_j - n_i))/(S_j/(96 - n_j)]$ follows a F distribution with $(n_j - n_i)$ and $(96 - n_j)$ degrees of freedom (Hays 1988). The null hypothesis that $S_i = S_j$ was then tested against the alternative $S_j < S_i$ at the 0.01 level.

At the sample level, individual F values were compared with the Kolmogorov-Smirnov test (see Desmurget et al. 2000).

TABLE 1. *Four classes of models for identifying the components of the vector errors*

Error Component	Model	Equation
Initial position	**Translation**	$(x_p,y_p) = (x_0,y_0) + (\tau,\upsilon)$
Direction-independent amplitude	Gain	$A = \alpha \times d$
	Affine	$A = \gamma \times d + \beta$
	Quadratic	$A = \gamma \times d - \beta \times d^2$
	Logarithmic	$A = \gamma/\beta \times \mathrm{Log}\,(1 + \beta \times d)$
	Exponential	$A = \gamma \times d^{\beta}$
Directional	**Rotation**	$D_m = D - \delta$
	Amplitude-dependent rotation	$D_m = D - \delta - \gamma \times d$
Direction-dependent amplitude	**Elliptic**	$A = d \times (1-\varepsilon^2)^{1/4}/(1-\cos^2(\theta-D_m)\varepsilon^2)^{1/2}$

Greek symbols in the equations identify the parameters of the corresponding model. Models were tested twice: by fitting a unique set of parameters to the data for both initial positions and by fitting the models separately to the data for each initial position. Initial-position error component: (x_0,y_0), (x_p,y_p), actual and represented initial position of the hand; (τ, υ), initial-position bias. Direction-independent amplitude error component: *A,* movement amplitude; *d,* distance of the target from the represented initial hand position; α, visuomotor gain. Directional error component: D_m, movement direction; *D*, target direction with respect to the represented initial hand position; δ, directional bias. Direction-dependent amplitude error component: ε, eccentricity of the ellipse; θ, inclination of the major axis of the ellipse. In this model, the ellipse is constrained to have the same surface of the unitary circle. Boldfaces identify the specific models that proved most satisfactory.

Under the null hypothesis, each individual *F* value is drawn independently from a *F* distribution with $n_j - n_i$ and $96 - n_j$ df. Thus the null hypothesis was rejected if the Kolmogorov-Smirnov test rejected (at the 0.01 level) the hypothesis that the sample of the individual *F* values is distributed as $F(n_j - n_i, 96 - n_j)$. Among alternative models with the same number of parameters, all significantly better than a model with a smaller number of parameters, we chose the one yielding the highest Kolmogorov-Smirnov statistic.

Initial-position biases

Initial-position biases were the major factor of inaccuracy, both at the sample and individual level. Following the stepwise strategy outlined in the preceding text, we began by testing the translation model (Table 1). The one-fit approximation (1 bias for both hand initial positions) reduced significantly the SSE in all but one subject (*MO*). The significance of the reduction was confirmed at the sample level [Kolmogorov-Smirnov (ks) test] where the total SSE (sum of individual SSEs) was decreased to 61.3% of its initial value (Table 2). The two-fit procedure (a different bias for each initial position) afforded a significantly larger reduction in six subjects. At the sample level, the effect was also significant, the total SSE being reduced to 54.1% of its initial value. This shows that initial-position biases depended on the initial position. As stressed before, such dependence is consistent with the VP hypothesis, insofar as the ability to estimate the position of the hand in the dark may vary with the posture of the arm.

Scaling biases

Scaling biases also represented a major source of inaccuracy both at the sample and individual level. To take into account this component, we considered five types of transformation of hand-target distance into movement amplitude (Table 1). In the simplest case (gain model), errors derive from multiplying by a constant visuomotor gain α the target distance predicted by the translation model. The second error model (affine model) generalizes the gain model by adding a constant term. The last three models correspond to more general, nonlinear, relationships between target distance and movement amplitude. These four models cover the main forms of relationship not captured by the gain model.

As for the gain model, $A = \alpha \times d$, the individual SSE was reduced significantly (with respect to the value obtained with the 2-fit translation model) in six subjects (range: 8–84%, Table 3, *1st column*). In these subjects, the visuomotor gain α was either smaller (4 individuals) or larger (2 individuals) than 1 (Fig. 5). At the sample level, the improvement was confirmed (ks = 0.676, $P < 0.0001$), the additional reduction (25.7%) decreasing the unaccounted SSE to 28.4% (54.1 − 25.7%). However, the gain model failed to account for a slight but consistent range effect: the predicted amplitude tended to be smaller (larger) than the actual one for close (far) targets. The effect was captured by more complex models than the gain model.

In six subjects, each of the four distance-dependent models improved significantly over the gain model (1-fit tests, Table 3 reports the comparison for the affine model). The same conclusion was reached at the sample level. However, we retained the affine model $A = \gamma \times d + \beta$ because, with respect to the gain model, it yielded a higher level of significance for the

TABLE 2. *Statistical analysis of error components (population)*

Error Model	df	ks	*P*	SSE	Red, %
Translation					
One fit	2,94	0.900	$<10^{-4}$	61.3	38.7
Two fit	2,92	0.675	$<10^{-4}$	54.1	7.2
Affine					
One fit	1,90	0.798	$<10^{-4}$	25.1	29.0
Two fit	2,88	0.227	>.60	24.8	0.3
Rotation					
One fit	1,89	0.868	$<10^{-4}$	21.4	3.7
Two fit	1,88	0.285	>.30	20.8	0.6
Elliptic					
One fit	2,87	0.601	.0005	19.9	1.5
Two fit	2,85	0.350	>.10	19.3	0.6

For each error component, the results when the parameters of the corresponding models are estimated simultaneously (1-fit), and separately (2-fit) for the two initial positions (recall that each model includes the previous ones) are reported. Two-fit models (e.g., rotation) are compared to the corresponding one-fit models. One-fit models (e.g., affine) are compared to the previous significant model (e.g., 2-fit translation). df, degrees of freedom of the Fisher *F* distribution used for individual tests; ks, Kolmogorov-Smirnov statistic assessing whether the sample of individual results is likely to be drawn from the predicted Fisher distribution (see text); *P*, probability associated to the Kolmogorov-Smirnov statistic. SSE, sum of square of the residuals (percent of the initial value); Red, reduction of the SSE afforded by the model.

TABLE 3. *Statistical analysis of amplitude errors (individual)*

	Gain Model		Affine Model	
Subject	One Fit	Two Fit	One Fit	Two Fit
BJ	8.00**	0.37 ns	14.22**	0.53 ns
CP	50.30**	0.53 ns	10.92*	1.47 ns
DC	42.80**	0.99 ns	25.10**	2.37 ns
IC	40.49**	0.05 ns	9.69*	0.41 ns
KA	0.64 ns	1.43 ns	0.00 ns	1.61 ns
KO	20.16**	0.03 ns	3.13 ns	0.54 ns
MO	84.00**	1.18 ns	0.13 ns	4.71 ns
PL	0.32 ns	0.18 ns	11.67**	1.64 ns
SM	0.40 ns	0.46 ns	2.82 ns	2.51 ns
VS	1.76 ns	0.30 ns	19.14**	0.50 ns
Average	24.89	0.55	9.68	1.63
Random	1.09	1.10	1.10	2.22

Percentage of individual SSE reduction (F test; *$P < 0.01$; ** $P < 0.001$). Values for two-fit models are relative to the SSE for the corresponding one-fit models. Values for the one-fit gain model are relative to the two-fit translation model; values for the one-fit affine model are relative to the one-fit gain model. Note that average values across subjects are relative to the residuals of the reference indicated above, not to the initial SSE, as in Table 2. Random: values expected in the absence of any effect (ratio of the degrees of freedom in the F statistics). For both models, the SSE explained by independent fits (columns 2 and 4) is much smaller, and never significantly higher than the SSE explained by a single fit.

sample test (ks = 0.690, $P = 0.00003$) than the three nonlinear models (exponential: ks = 0.628, $P = 0.00024$; logarithmic: ks = 0.593, $P = 0.00070$; quadratic: ks = 0.589, $P = 0.00077$). With respect to the gain model, the unaccounted SSE was reduced by an additional 3.3%. The affine model can be expressed as $A = \alpha \times d_m + \gamma \times (d–d_m)$ where α is the same visuomotor gain that appears in the gain model and d_m is the average represented hand-target distance. This formulation affords a natural interpretation of the parameter γ as a contraction/extension rate (McIntyre et al. 2000), which modulates a default average amplitude $A_m = \alpha \times d_m$ (Ghez et al. 1997; Hening et al. 1988; Pellizzer and Hedges 2004). Values of $\gamma < 1$ signal the classical range effect (Slack 1953), i.e., a central tendency bias. The affine model can also be written in the form $A = \alpha \times d + (\gamma–\alpha) \times (d–d_m)$. The term $(\gamma–\alpha) \times (d–d_m)$ added to the gain model represents a *relative* range effect with respect to the end points predicted by the visuomotor gain alone. The individual one-fit values of the parameters α and γ are plotted against each other in Fig. 5, showing that a variable amount of range effect was present in all subjects. The affine model was significantly more accurate than the gain model in six subjects (data points with the greatest vertical distance from the diagonal in Fig. 5). Note that in all but one subject, the extension/contraction rate was smaller than the visuomotor gain, indicating that the amplitude difference between movements to the furthest and closest targets was generally smaller than predicted by the gain model alone.

The VP hypothesis bars scaling biases from depending on the initial hand position. This crucial prediction was confirmed statistically. Allowing the parameters of the affine model to depend on the initial position reduced by at most 4.71% the SSE left unaccounted by the one-fit procedure (*subject MO,* Table 3, *4th column*). Even in this case, the reduction, which was small with respect to the initial SSE (0.8%), did not reach significance [$F(2,88) = 2.17$, $P > 0.10$]. Moreover, the sample statistics also failed to detect significant differences between starting positions (Table 2). Similar negative results were obtained with the exponential, logarithmic and quadratic models. We tested the independence of scaling biases from the initial position also with the gain model, which, although less accurate than the affine model, afforded a large reduction of the SSE. As shown in Table 3, allowing the visuomotor gain to depend on the starting position failed to improve the fitting with respect to using a single gain. The further reduction of the SSE (Table 3, *2nd column*) ranged from 0.03 to 1.43% and was not significant either at the sample (ks = 0.257, $P > 0.45$) or the individual level (in all cases, $P > 0.25$). Averages in Table 3 show that adding 1 df to the gain model by letting the parameter α depend on the initial position reduced the SSE far less (0.55%) than by adding the parameter γ to obtain the affine model (1 fit, 9.68%).

Directional biases

Directional biases represented a limited but still highly significant source of inaccuracy, both at the individual and sample level. There was a counterclockwise bias in all subjects (range: 1.1–6.6°), which reached significance ($P = 0.001$) in six cases. At the sample level, 3.7% of the total SSE was captured by the rotation model, which added a constant angle to the hand-target direction predicted by the affine model. We tested whether directional biases depended on the initial position. At the individual level, differences between direction errors from the two initial positions were idiosyncratic, the SSE being reduced significantly only in one subject (*BJ*). At the sample level, allowing a different directional bias for each initial position did not improve the fit significantly with respect to the one-fit procedure (Table 2). We also tested the hypothesis that directional biases depend on target distance through an affine (2 parameter) function. The SSE reduction afforded by the additional degree of freedom did not attain statistical significance either at the individual or sample level.

Inertia-dependent amplitude biases

If unaccounted residuals were due to the anisotropy of the arm inertia, their distribution should be roughly elliptical with over-

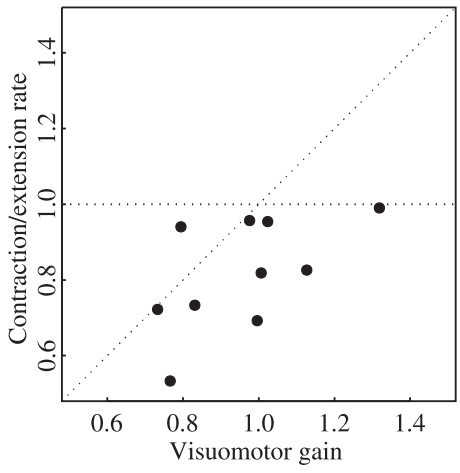

FIG. 5. Scaling biases. Relation between the visuomotor gain α (abscissa) in the gain model and the contraction/extension rate γ (ordinate) in the affine model. Data points are best-fit estimates based on individual results. Subjects could be hypometric (4 leftmost points), orthometric (4 middle points), or hypermetric (2 rightmost points). The parameter γ represents a gain acting on the difference between target distance and average target distance. Its effect adds to that of the global gain α (see text). In all cases, γ was smaller than 1, indicating some degree of range effect (central tendency bias).

and under-shootings aligned with the shortest and longest axis of inertia of the arm, respectively. Also, peak velocity and peak acceleration should exhibit a similar directional modulation, while movement duration should be longest (shortest) for movements along the longest (shortest) axis of inertia (Gordon et al. 1994a). Finally, the orientation of the ellipses should depend on the starting location because the anisotropy of the inertia depends mainly on the orientation of the forearm at the onset of the movement. With our experimental apparatus, the longest axis of the ellipses for amplitude, peak velocity, and peak acceleration should rotate clockwise from ~50° for movements from the left initial position to ~20° for movements from the right initial position.

We applied an elliptic, direction-dependent modulation of amplitude to the vectors predicted by the combination of initial-position, scaling, and directional biases (elliptic model in Table 1). We began by assuming that the two parameters of the model are independent of the initial position (1 fit). Adding this source of error resulted in a significant reduction of the individual SSE in four subjects. The improvement was confirmed at the sample level (Table 2). Fitting the parameters of the model separately for each initial position (2 fit) did not reduce significantly the SSE either at the individual or sample level (Table 2). The failure to improve the fitting is inconsistent with the assumption of an inertia-dependent amplitude bias because the distribution of the masses was different for the two initial positions. The two-fit elliptic model involves 11 independent parameters [4 (translation) + 2 (affine) + 1 (rotation) + 4 (elliptic)]. Therefore the failure may be due to the fact that differences between errors were too small with respect to the complexity of the parameter space.

The role of inertia was scrutinized further by examining how amplitude, movement duration, and peak values of velocity and acceleration varied as a function of movement direction. The analysis involved several steps. Velocity, acceleration, and duration covaried with movement amplitude. To pool the data for all targets, the first step was to eliminate this dependency by fitting cubic functions to the relationships between amplitude and kinematic parameters. The procedure was performed independently for each initial position and each subject. Amplitudes were also normalized for each movement. They were divided by the value predicted by the model incorporating initial-position, scaling, and directional biases and multiplied by the average amplitude over all trials. In the second step, individual data were linearly transformed to equalize means and SDs of each kinematic variable. Because of the relative scarcity of the individual data, we pooled separately the results from the five subjects with the largest directional modulation of amplitude, and those from the other five subjects. In the first group (Fig. 6, *left*), peak acceleration exhibited a clear directional modulation (eccentricity of the best-fitting elliptic approximation to the data points ≅0.70, i.e., a major-to-minor axis ratio of 1.4), with peaks along the 46 and 17° directions for the left and right initial position, respectively. The results were similar for peak velocity (47 and 13°), maximum amplitude (49 and 10°), and movement duration (135 and 101°; note that the direction of the peaks for duration are rotated by 90°). A similar pattern emerged for the other group (Fig. 6, *right*). The axes along which peak acceleration, and peak velocity were largest (and the duration was shortest) were almost the same as in the first group (43 and 15, 48 and 19, 129 and 104°, respectively). The modulation of movement amplitude was too

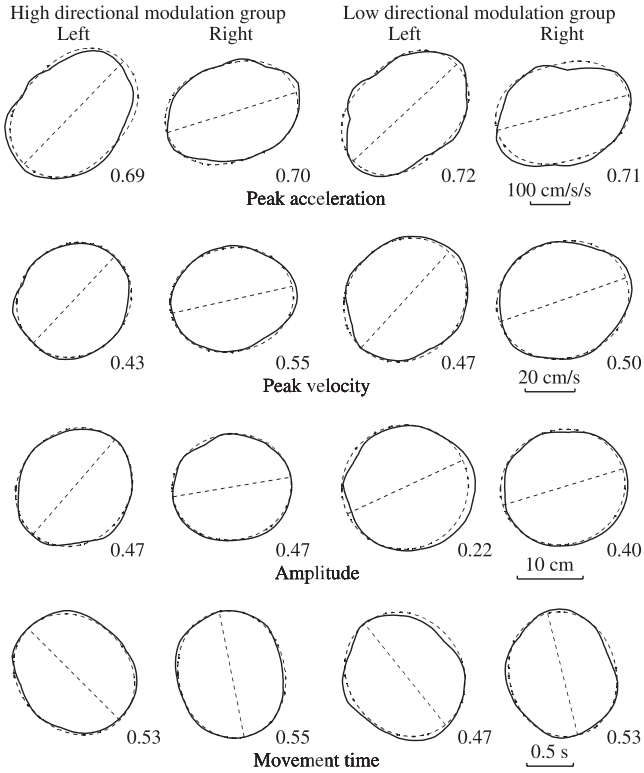

FIG. 6. Direction-dependent modulation of kinematic parameters. The *two leftmost* and the *two rightmost columns* report the average results over 2 equal groups of subjects (see text). Left/right: initial positions. Each row is relative to the indicated kinematic parameter averaged over target distance. Continuous lines: interpolation of the data points by a robust local smooth. Dashed lines: elliptic interpolation of the same data. Direction and extent of the modulation are estimated by the orientation of the major axis, and by the indicated eccentricity of the ellipses. In both groups, the directions of maximum modulation for acceleration and velocity are consistent with the orientation of the axis of least inertia of the arm in the posture adopted for the indicated initial position. Movement duration is longest in the direction for which the other kinematic parameters are smallest. Note that the 2 groups differ only in the average modulation of amplitude.

weak to provide a reliable estimate of the rotation angle for the left initial position. In conclusion, although the reduction of the SSE obtained by allowing the parameters of the elliptic model to depend on the initial position failed to reach statistical significance, the anisotropy of the arm inertia did indeed modulate the kinematics of the movements.

Unaccounted residuals

Figure 7 illustrates the effectiveness of the final model—which integrates the assumed sources of bias—by comparing the population distribution of the pointing errors with the distribution of the unaccounted residuals. However, in spite of the massive reduction of the errors, the residuals were not distributed randomly. For each target separately, we tested whether the mean of the residuals was different from zero (Hotelling's T^2 statistic) (Morrison 1976). Assuming that the residuals for all 10 subjects were drawn from a Gaussian bivariate distribution, the set of the 10 individual residuals should be such that the statistic $F = (10 - 2)/(10 - 1)/2 \times T^2$ follow a Fisher $F(2,8)$ distribution. In essence, we tested whether the predicted end point was within the between-subjects 95% confidence ellipse centered on the average end point. For 10 of the 48 targets (dotted-line ellipses) the mean

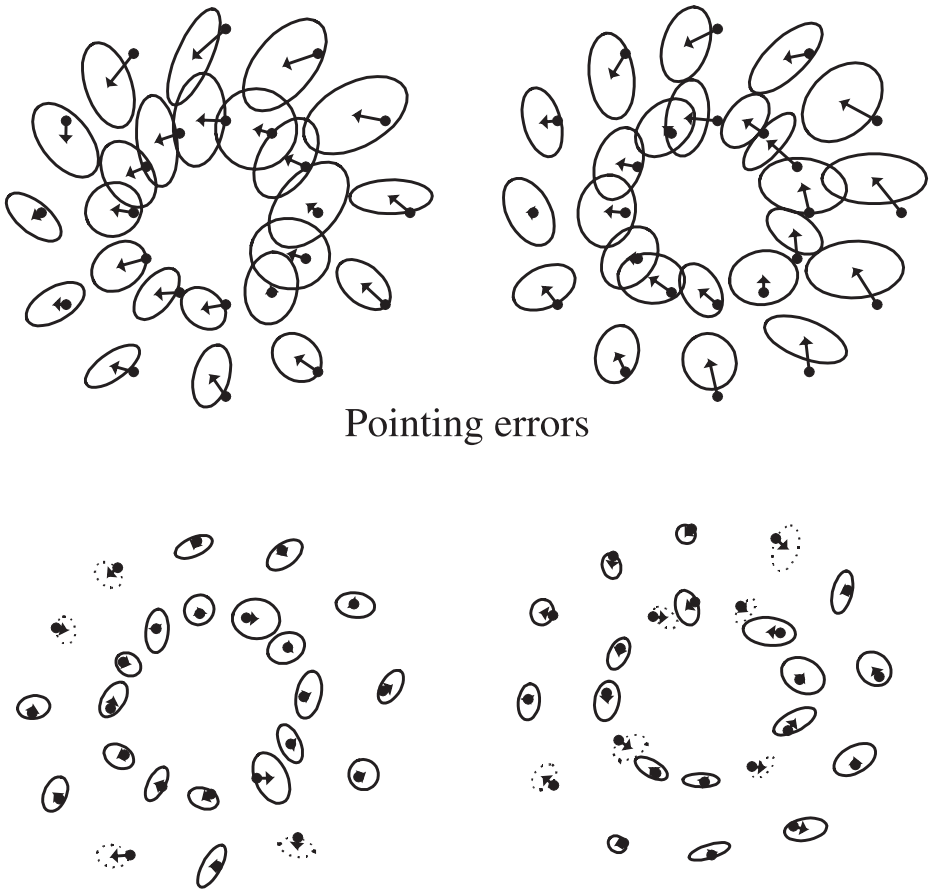

FIG. 7. Reduction of inter-individual variability. *Top*: error vectors connecting targets (dots) to the actual final positions (averaged over all trials and all subjects). The variability across subjects is described by 95% tolerance ellipses. For graphic clarity, the data for the left and right initial positions were separated. *Bottom*: vectors (unaccounted residuals) connect the final positions predicted by the Elliptic model (dots) to the actual final positions (averages across subjects). Note that in 10 cases (dotted-line ellipses), there is a significant ($P < 0.05$) difference between actual and predicted final position, suggesting target-dependent sources of error not captured by the model.

residuals were significantly different from 0 ($P < 0.05$). Then, using the ks test, we compared the 48 F values defined above with the theoretical $F(2,8)$ distribution corresponding to the hypothesis that, for all targets, the residuals for each subject are independent bivariate Gaussian variables. This global analysis confirmed that residual errors were not distributed randomly [$F(2,8)$, ks = 0.247, $P < 0.005$]. Therefore even the final nine-parameter elliptic model left unaccounted a source of target-dependent errors.

Individual variability

Figure 8 shows for each subject the total SSE and the relative contributions of the three sources of inaccuracy captured by the translation, rotation, and elliptic models and of the two sources captured by the affine model (visuomotor gain and relative range effect). The proportion of unaccounted residuals ranged from 11% for *subject KO* to 43% for *subject VS.* Moreover, also the balance among types of residuals differed considerably across subjects. Two points are worth emphasizing. First, the pointing errors made by the subjects with the largest proportion of unaccounted residuals were rather unsystematic (*VS* and *BJ,* Fig. 9) and did not suggest an alternative to the VP hypothesis. Second, the smallest proportions of residuals were observed for the least accurate subjects (*DC* to *KA,* Fig. 8). Thus the absolute amount of unexplained residuals was not dramatically different across subjects. In other words, idiosyncratic amounts of initial-position, scaling, directional, and inertia-dependent biases were added to a fairly constant amount of random variability.

Are our data compatible with an alternative positional model?

So-called positional (or postural) models hold that movements are planned by specifying either a point of equilibrium among muscle synergies (Bizzi et al. 1992; Feldman 1986) or the final posture to be reached (Graziano et al. 2002; Rosenbaum et al. 1993). In sharp contrast with the VP hypothesis, these models predict that end-point errors depend only on the target location not on the hand-target vector. This prediction was tested by focusing on five targets, namely the common target C (Fig. 1), and the two pairs of symmetrical targets just above and below C. Positional models predict a positive correlation between the x coordinates of the errors both for movements to the same target from opposite initial positions and for movements to close targets from the same initial position. In the first case, the predictions of the VP hypothesis depend on the balance between initial-position biases on the one side, and scaling, directional, inertia-dependent biases, on the other. When the former prevail, one expects again a positive correlation, because errors on the initial positions are positively correlated (Vindras et al. 1998). When the latter prevail, errors should show a negative correlation. For example, an hypometric subject would make leftward errors from the left initial position and rightward errors from the right initial position. Therefore in contrast with positional models, the VP hypothesis predicts negative correlations when the initial-position biases are corrected. Table 4 (*1st 3 lines*) reports the correlation coefficients at the three indicated stages

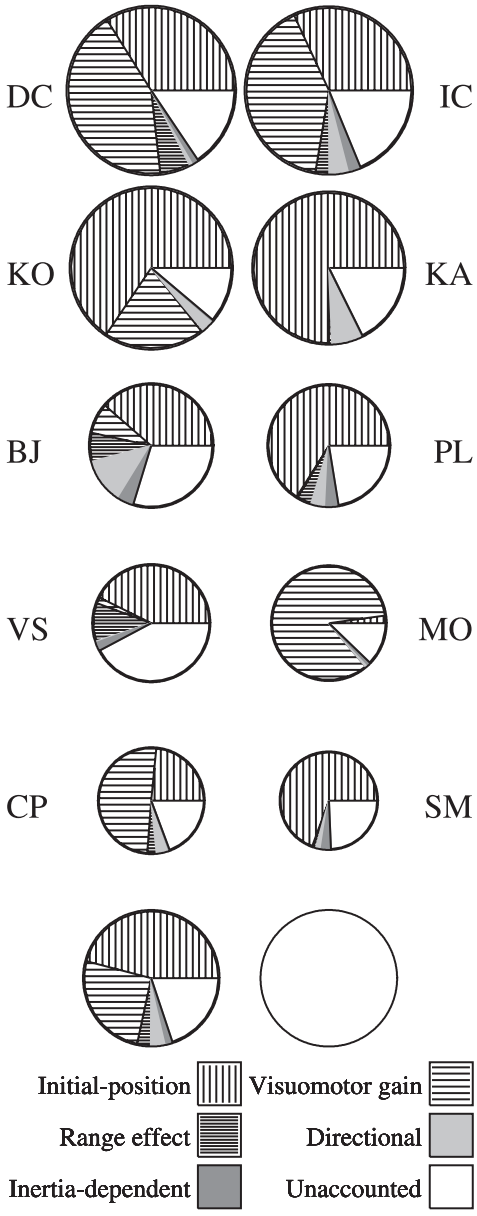

FIG. 8. Relative weight of the error components for all subjects. The initial SSE is represented by the area of the circular histogram. The relative weight of the components varies across subjects. *Bottom*: average across subjects (*left*) and calibration (root mean square error = 3.3 cm).

of error modeling. For the reason explained in the preceding text, the tendency for original errors associated with opposite movements to mirror each other (*1st column*) suggest that scaling, directional, and inertia-dependent biases prevail. More importantly, the strong negative correlations between x components after taking into account initial-position biases (*2nd column*) shows clearly the symmetry between errors for left- and rightward movements. Note that correlations disappear after taking into account all error components (*3rd column*), which confirms that residuals were independent of the movement characteristics. As for movements from the same initial positions to nearby targets (*4 last lines* in Table 4), both the VP hypothesis and positional models predict positive correlations. However, only the VP hypothesis predicts the opposite signs of

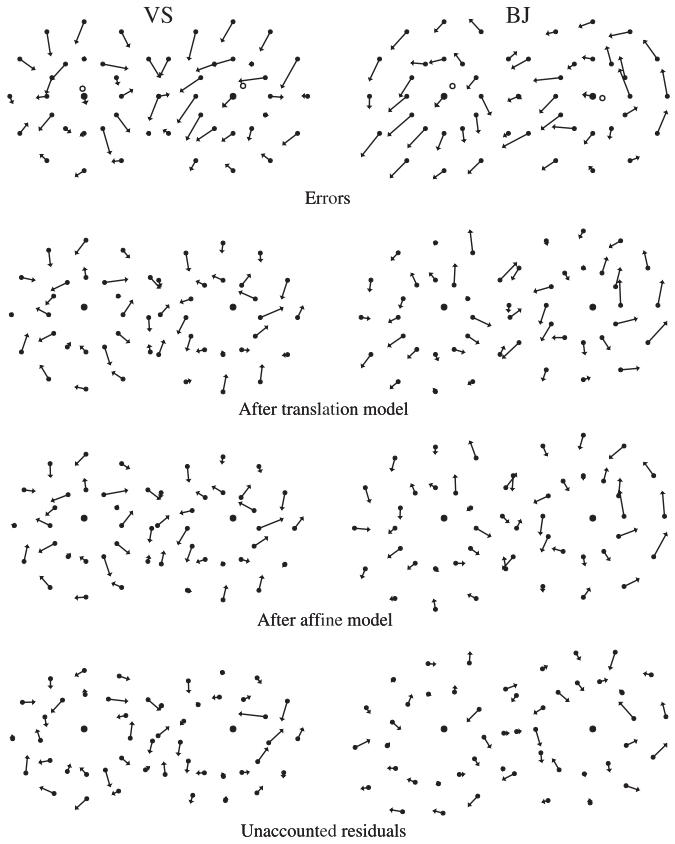

FIG. 9. Modeling the errors. Data for the 2 subjects with the largest amount of unaccounted residuals. *Top*: vectors from targets to actual end points. *Bottom 3 rows*: vectors from predicted to actual end points. Note that unaccounted residuals do not follow any systematic pattern.

the correlation between movements from the same or different initial positions (*2nd column*). In summary, the analysis of the errors for the five selected targets clearly favored the VP model over positional models.

TABLE 4. *Error correlations*

Movements	Original Errors	Without Initial-Position Biases	Unaccounted Residuals
Opposite initial position			
Target C	−0.715	−0.855*	+0.163
Targets above C	−0.539	−0.786*	−0.008
Targets below C	−0.322	−0.861*	−0.161
Left initial position			
Target C/target above C	+0.919**	+0.856*	+0.034
Target C/target below C	+0.964**	+0.924**	+0.525
Right initial position			
Target C/target above C	+0.658	+0.813*	−0.244
Target C/target below C	+0.809*	+0.845*	−0.324

Correlation between the x coordinates of errors for movements towards the common target C from opposite initial positions (lines 1–3), and towards adjacent targets (above or below C) from the same initial positions (lines 4–7). Results for the original errors, the residuals of the translation model (2-fit), and the unaccounted residuals (elliptic model, 1-fit); *$P = 0.01$; ** $P = 0.001$. The hypothesis that errors depend on target position, but not on the initial position, predicts positive correlations in all cases. The vectorial parametric hypothesis predicts negative correlations for the *second column* (1st 3 lines), positive correlations for the *first two columns* of the four last lines, and no correlation for the unaccounted residuals.

DISCUSSION

We provided evidence that the pattern of end-point errors in a two-dimensional pointing task is consistent with the VP hypothesis that movements are planned in a hand-centered coordinate system with direction and extent of the movement as independently controlled parameters. Errors compounded five sources of inaccuracy: *1*) an initial-position bias, which was the most conspicuous one (46% of the total SSE explained by 4 parameters). The corresponding error component varied as a function of the initial position in the same way as the bias in the perceptual estimation of the initial hand location (Vindras et al. 1998). *2*) A scaling bias (29% of the total SSE, 2 parameters), which was dependent on target distance, but independent of both the initial position and the direction of the movement. This bias could be factored out in two terms. The most conspicuous one (25.7%, 1 parameter), proportional to target distance, was due to an inaccurate visuomotor gain. The second term (3.3%, 1 parameter) modulated the visuomotor gain in agreement with the well-known range effect. *3*) A directional bias (3.7%, 1 parameter) characterized by a counterclockwise pointing bias independent of both initial position and target distance. *4*) An amplitude modulation related to the tensor of inertia of the arm (1.5%, 2 parameters). These five principled sources of error, incorporated in a single model, predicted well the actual movements by fitting the 96 errors coordinates with only 9 parameters (<20% of the sample SSE was left unaccounted, see Table 2). Moreover, in the two subjects (*BJ* and *VS*) for whom the unaccounted SSE was >25% (Fig. 8), the unaccounted residuals failed to display any regularity (Fig. 9).

All types of errors yielding a significant reduction of the SSE were in keeping with the VP hypothesis. Conversely, all types of errors at variance with the VP hypothesis failed to improve significantly the predicted final positions. The analysis of amplitude errors provided direct support to the hypothesis insofar as a single set of parameters for both initial positions was sufficient to capture the inaccuracies related to target distance. Indeed (Table 3), the improvement afforded by letting the parameters of both the gain and affine models to depend on the initial position was below chance level.

The modeling of the movement proved quite successful in that the residuals were much smaller than the original errors (Fig. 7). However, for some targets, the mean residual across subjects was still significantly different from zero. One likely reason for these discrepancies is that all models included an error term affecting the represented hand position but not an error term affecting the represented position of the targets. Clearly, this is an oversimplification. Indeed, several authors have reported direction-dependent directional errors causing the movement to rotate away from the four cardinal directions (Ghez et al. 1993; Ghilardi et al. 1995; Graaf et al. 1991, 1994; Smyrnis et al. 2000). These errors are supposed to reflect a perceptual distortion in the estimation of the target location (Gourtzelidis et al. 2001; Graaf et al. 1996; Huttenlocher et al. 1991). Some of the significant residuals suggest a similar tendency for the end points to move away from the vertical axis (Fig. 7). Note, however, that errors on target location are neither conflicting with, nor predicted by, the VP hypothesis.

Our analyses focused on the constant errors, which so far have proved less discriminating than the variable errors (e.g., McIntyre et al. 1998). There were two reasons why our strategy was more successful. On the one side, unlike most previous studies, we tested a large array of symmetric targets. In particular, using circular arrays of targets at various distances around two initial positions was instrumental for sorting out the different sources of inaccuracy. If fewer, nonsymmetrical targets had been used, some of the results would have been ambiguous. For instance, considering only the six targets located at 150, 180, and 210° would have led to the conclusion that *subject KO* had a systematic tendency toward overshooting, whereas using the six targets located at –30, 0, and 30° would have led to the opposite conclusion (Fig. 4*C,* left initial position). On the other side, the analysis was conducted mainly at the individual level, allowing us to capture the idiosyncratic components of the performance. This is seen most clearly in the case of the visuomotor gain. Performing a classical statistical analysis only at the sample level would have led to the conclusion that the average visuomotor gain was not different from 1 ($t_9 = -1.13$; $P > 0.25$). In fact, individual gains ranged from 0.73 to 1.28 (Fig. 5) and were significantly different from 1 ($P < 0.001$) in two hypermetric and four hypometric subjects. Using a Kolmogorov-Smirnov test, we were able to show that the null hypothesis (gain = 1) could be rejected also at the sample level.

The main support for the VP hypothesis comes from experiments involving pointing movements in the horizontal plane (Bock and Eckmiller 1986; Brown et al. 2003; Desmurget et al. 1997; Ghez et al. 1997; Rossetti et al. 1995; Vindras and Viviani 1998). Instead, the results of several studies involving three-dimensional (3D) arrays of targets are at variance with the hypothesis. Specifically, it was reported that the ellipsoids describing end-point variability are oriented either toward the eye (Carrozzo et al. 1999; McIntyre et al. 1997; van den Dobbelsteen et al. 2001) or toward the shoulder (Adamovich et al. 1998; Baud-Bovy and Viviani 1998). In either case, these analyses of the variable error are more in keeping with the postural control view evoked in the INTRODUCTION than with the VP hypothesis, which predicts that the ellipsoid is oriented toward the initial position of the hand. Likewise, the analysis of the constant errors led some authors (e.g., van den Dobbelsteen et al. 2001) to suggest that the motor system uses only the intended final position to control simple 3D movements. Other authors (Desmurget and Prablanc 1997; Flanders et al. 1992; Rosenbaum et al. 1995) favor instead the hypothesis that movements are driven toward a target posture.

It is not clear why 2D and 3D studies lead to conflicting conclusions. At least three factors may be responsible for the disagreement. First, it is generally admitted (Abrams et al. 1994; de Grave et al. 2004; Feldman and Levin 1995; Ghez 1979; Gottlieb 1996; McIntyre and Bizzi 1993; Sainburg et al. 1999) that all pointing movements involve the concomitant planning of a transport phase and of a final stabilization phase. However, in the case of 3D movements, the stabilization of the final arm posture is likely to affect end-point errors to a greater extent than in the case of movements in the horizontal plane because gravity must be compensated for in the former but not in the latter situation. Second, in most 2D studies, unlike their 3D counterparts, subjects are encouraged to produce one-shot, uncorrected movements. Thus the distribution of end points in 2D tasks is likely to reflect mainly the contribution of the transport phase, whereas in 3D tasks, it is likely to reflect

mainly the contribution of the stabilization phase. Third, the position of 3D visual targets is generally affected by a greater uncertainty than that of 2D targets because only in the former case depth information must be taken into account. Thus at least in the case of visual targets, it is possible that errors in the stored representation of the eye-target distance (McIntyre et al. 1997, 1998) dominate the errors generated by motor processes. If so, one should be cautious in drawing conclusions about these processes on the sole basis of the orientation of the ellipsoids of variability (Admiraal et al. 2003).

One final point concerning the origin of the system of reference involved in movement planning. Some authors have argued that movements are planned within a gaze-centered representation (Batista et al. 1999; Buneo et al. 2002; Crawford et al. 2004; Henriques et al. 1998). Because in pointing tasks subjects are likely to fixate the target during the planning phase, this view may be equivalent to assume a target-centered frame of reference. For the purpose of this discussion, it should be stressed that the alignment of the initial and final positions with the target is totally independent of the origin of the reference. Therefore our results are fully compatible with the view that movements are planned in a gaze-centered rather than hand-centered representation. Of course, the issue cannot be adjudged on the sole basis of kinematic data. Resolving it may require an independent control of the gaze orientation before movement inception (Henriques et al. 1998). It should be stressed, however, that the question of the origin of the system of reference does not bear on the crucial tenet of the VP hypothesis, namely that amplitude and direction of the planned movement are processed separately.

ACKNOWLEDGMENTS

We thank C. Ghez and two anonymous reviewers for valuable remarks and suggestions.

GRANTS

This work was partly supported by Swiss National Fund Grant 3100–055620 to P. Viviani, and by research funds from the Vita-Salute San Raffaele University.

REFERENCES

Abrams RA, van Dillen L, and Stemmons V. Multiple sources of spatial information for aimed limb movements. In: *Conscious and nonconscious information processing. Attention and Performance XV,* edited by Umilta C and Moscovich M. Cambridge, MA: MIT Press, 1994, p. 1–20.

Adamovich SV, Berkinblit MB, Fookson OI, and Poizner H. Pointing in 3D space to remembered targets. I. Kinesthetic versus visual target presentation. *J Neurophysiol* 79: 2833–2846, 1998.

Admiraal MA, Keijsers NLW, and Gielen CCAM. Interaction between gaze and pointing toward remembered visual targets. *J Neurophysiol* 90: 2136–2148, 2003.

Atkeson CG and Hollerbach JM. Kinematic features of unrestrained vertical arm movements. *J Neurosci* 5: 2318–2330, 1985.

Batista AP, Buneo CA, Snyder LH, and Andersen RA. Reach plans in eye-centered coordinates. *Science* 285: 257–260, 1999.

Baud-Bovy G and Viviani P. Pointing to kinesthetic targets in space. *J Neurosci* 18: 1528–1545, 1998.

Bizzi E, Accornero N, Chapple W, and Hogan N. Posture control and trajectory formation during arm movement. *J Neurosci* 4: 2738–2744, 1984.

Bizzi E, Hogan N, Mussa-Ivaldi FA, and Giszter SF. Does the nervous system use the equilibrium point control to guide single and multiple joint movements. *Behav Brain Sci* 15: 603–613, 1992.

Bock O. Adaptation of aimed arm movements to sensorimotor discordance: evidence for direction-independent gain control. *Behav Brain Res* 51: 41–50, 1992.

Bock O and Arnold K. Motor control prior to movement onset: preparatory mechanisms for pointing at visual targets. *Exp Brain Res* 90: 209–216, 1992.

Bock O and Eckmiller R. Goal-directed arm movements in absence of visual guidance: evidence for amplitude rather than position control. *Exp Brain Res* 62: 451–458, 1986.

Brown LE, Rosenbaum DA, and Sainburg RL. Movement speed effects on limb position drift. *Exp Brain Res* 153: 266–274, 2003.

Buneo CA, Jarvis MR, Batista AP, and Andersen RA. Direct visuomotor transformations for reaching. *Nature* 416: 632–636, 2002.

Carrozzo M, McIntyre J, Zago M, and Lacquaniti F. Viewer-centered and body-centered frames of reference in direct visuomotor transformations. *Exp Brain Res* 129: 201–210, 1999.

Crawford JD, Medendorp WP, and Marotta JJ. Spatial transformation for eye-hand coordination. *J Neurophysiol* 92: 10–19, 2004.

Cruse H. Constraints for joint angle control of the human arm. *Biol Cybern* 54: 125–132, 1986.

de Grave DJD, Brenner E, and Smeets JBJ. Illusions as a tool to study the coding of pointing movements. *Exp Brain Res* 155: 56–62, 2004.

Desmurget M, Grafton ST, Vindras P, Gréa H, and Turner RS. The basal ganglia network mediates the planning of movement amplitude. *Eur J Neurosci* 19: 2871–2880, 2004.

Desmurget M, Jordan M, Prablanc C, and Jeannerod M. Constrained and unconstrained movements involve different control strategies. *J Neurophysiol* 77: 1644–1650, 1997.

Desmurget M and Prablanc C. Postural control of three dimensional prehension movements. *J Neurophysiol* 77: 452–464, 1997.

Desmurget M, Vindras P, Gréa H, Viviani P, and Grafton ST. Proprioception does not quickly drift during visual occlusion. *Exp Brain Res* 134: 363–377, 2000.

Feldman AG. Functional tuning of the nervous system during control of movement or maintenance of a steady posture. III. Mechanographic analysis of the execution by man of the simplest motor tasks. *Biophysics* 11: 766–775, 1966.

Feldman AG. Once more on the equilibrium-point hypothesis (lambda model) for motor control. *J Mot Behav* 18: 17–54, 1986.

Feldman AG and Levin MF. The origin and use of positional frames of reference in motor control. *Behav Brain Sci* 18: 723–806, 1995.

Flanders M, Helms Tillery SI, and Soechting JF. Early stages in sensorimotor transformations. *Behav Brain Sci* 15: 309–362, 1992.

Ghez C. Contributions of central programs to rapid limb movements in the cat. In: *Integration in the Nervous System,* edited by Asanuma H and Wilson VJ. Tokyo: Igaku-Shoin, 1979, p. 305–320.

Ghez C, Favilla M, Ghilardi MF, Gordon J, Bermejo J, and Pullman S. Discrete and continuous planning of hand movements and isometric force trajectories. *Exp Brain Res* 115: 217–233, 1997.

Ghez C, Gordon J, and Ghilardi MF. Programming of extent and direction in human reaching movements. *Biomed Res* 14: 1–5, 1993.

Ghilardi MF, Gordon J, and Ghez C. Learning a visuo-motor transformation in a local area of work space produces directional biases in other areas. *J Neurophysiol* 73: 2535–2539, 1995.

Gordon J, Ghilardi MF, Cooper SE, and Ghez C. Accuracy of planar reaching movements. II. Systematic extent errors resulting from inertial anisotropy. *Exp Brain Res* 99: 112–130, 1994a.

Gordon J, Ghilardi MF, and Ghez C. Accuracy of planar reaching movements. I. Independence of direction and extent variability. *Exp Brain Res* 99: 97–111, 1994b.

Gottlieb GL. On the voluntary movement of compliant (inertial-visco-elastic) loads by parcellated control mechanisms. *J Neurophysiol* 76: 3207–3229, 1996.

Gourtzelidis P, Smyrnis N, Evdokimidis I, and Balogh A. Systematic errors of planar arm movements provide evidence for space categorization effects and interaction of multiple frames of reference. *Exp Brain Res* 139: 59–69, 2001.

Graaf JBd, Denier van der Gon JJ, and Sittig AC. Vector coding in slow goal-directed arm movements. *Percept Psychophys* 58: 587–601, 1996.

Graaf JBd, Sittig AC, and Denier van der Gon JJ. Misdirections in slow goal-directed arm movements and pointer- setting tasks. *Exp Brain Res* 84: 434–438, 1991.

Graaf JBd, Sittig AC, and Denier van der Gon JJ. Misdirections in slow, goal-directed arm movements are not primarily visually based. *Exp Brain Res* 99: 464–472, 1994.

Graziano MSA, Taylor CSR, and Moore T. Complex movements evoked by microstimulation of precentral cortex. *Neuron* 34: 841–851, 2002.

Hays WL. *Statistics.* Orlando, FL: Holt, Rinehart and Winston, 1988.

Hening W, Favilla M, and Ghez C. Trajectory control in targeted force impulses. V. Gradual specification of response amplitude. *Exp Brain Res* 71: 116–128, 1988.

Henriques DYP, Klier EM, Lowy D, and Crawford JD. Gaze-centered remapping of remembered visual space in an open-loop pointing. *J Neurosci* 18: 1583–1594, 1998.

Huttenlocher J, Hedges LV, and Duncan S. Categories and particulars: prototype effects in estimating spatial location. *Psychol Rev* 98: 352–376, 1991.

Krakauer JW, Pine ZM, Ghilardi MF, and Ghez C. Learning of visuomotor transformations for vectorial planning of reaching trajectories. *J Neurosci* 20: 8916–8924, 2000.

McIntyre J and Bizzi E. Servo hypotheses for the biological control of movement. *J Mot Behav* 25: 193–202, 1993.

McIntyre J, Stratta F, Droulez J, and Lacquaniti F. Analysis of pointing errors reveals properties of data representations and coordinate transformations within the central nervous system. *Neural Comput* 12: 2823–2855, 2000.

McIntyre J, Stratta F, and Lacquaniti F. Viewer-centered frame of reference for pointing to memorized targets in three-dimensional space. *J Neurophysiol* 78: 1601–1618, 1997.

McIntyre J, Stratta F, and Lacquaniti F. Short-term memory for reaching to visual targets: psychophysical evidence for body-centered reference frames. *J Neurosci* 18: 8423–8435, 1998.

Messier J and Kalaska JF. Comparison of variability of initial kinematics and endpoints of reaching movements. *Exp Brain Res* 125: 139–152, 1999.

Morrison DF. *Multivariate Statistical Methods.* New York: McGraw Hill, 1976.

Pellizzer G and Hedges JH. Motor planning: effect of directional uncertainty with continuous spatial cues. *Exp Brain Res* 154: 121–126, 2004.

Prablanc C, Pélisson D, and Goodale MA. Visual control of reaching movements without vision of the limb. I. Role of extraretinal feedback of target position in guiding the hand. *Exp Brain Res* 62: 293–302, 1986.

Rabiner LR and Gold R. *Theory and Application of Digital Signal Processing.* Englewood Cliffs, NJ: Prentice-Hall, 1975.

Rosenbaum DA. Human movement initiation: specification of arm direction and extent. *J Exp Psychol Gen* 109: 444–474, 1980.

Rosenbaum DA, Engelbrecht SE, Bushe MM, and Loukopoulos LD. Knowledge model for selecting and producing reaching movements. *J Mot Behav* 25: 217–227, 1993.

Rosenbaum DA, Loukopoulos LD, Meulenbroek RGJ, Vaughan F, and Engelbrecht SE. Planning reaches by evaluating stored postures. *Psychol Rev* 102: 28–67, 1995.

Rossetti Y, Desmurget M, and Prablanc C. Vectorial coding of movement: Vision, proprioception or both? *J Neurophysiol* 74: 457–463, 1995.

Sainburg RL, Ghez C, and Kalakanis D. Intersegmental dynamics are controlled by sequential anticipatory, error correction, and postural mechanisms. *J Neurophysiol* 81: 1045–1056, 1999.

Slack CW. Some characteristics of the range effect. *J Exp Psychol* 46: 76–80, 1953.

Smyrnis N, Gourtzelidis P, and Evdokimidis I. A systematic directional error in 2-D arm movements increases with increasing delay between visual target presentation and movement execution. *Exp Brain Res* 131: 111–120, 2000.

van den Dobbelsteen JJ, Brenner E, and Smeets JBJ. Endpoints of arm movements to visual targets. *Exp Brain Res* 138: 279–287, 2001.

Vindras P, Desmurget M, Prablanc C, and Viviani P. Pointing errors reflect biases in the perception of the initial hand position. *J Neurophysiol* 79: 3290–3294, 1998.

Vindras P and Viviani P. Frames of reference and control parameters in visuomanual pointing. *J Exp Psychol Hum Percept Perform* 24: 569–591, 1998.

Vindras P and Viviani P. Altering the visuo-motor gain: Evidence that motor plans deal with vector quantities. *Exp Brain Res* 147: 280–295, 2002.

Wann JP and Ibrahim SF. Does limb proprioception drift? *Exp Brain Res* 91: 162–166, 1992.